

Dramatic density-of-state enhancement of Raman scattering at the band edge in a one-dimensional photonic-crystal waveguide

Kuon Inoue,¹ Hisaya Oda,¹ Akio Yamanaka,¹ Naoki Ikeda,^{2,3} Hitoshi Kawashima,² Yoshimasa Sugimoto,² and Kiyoshi Asakawa³

¹*Chitose Institute of Science and Technology, 758-Bibi, Chitose, Hokkaido 066-8655, Japan*

²*National Institute of Advanced Industrial Science and Technology, Tsukuba, Ibaraki 305-8568, Japan*

³*Center for Tsukuba Advanced Research Alliance, University of Tsukuba, Tsukuba, Ibaraki 305-8577, Japan*

(Received 28 December 2007; published 18 July 2008)

We have measured the intensity of Raman scattering light, which is due to optical phonons, as a function of excitation laser wavelength for the guide-mode band of $\text{Al}_x\text{Ga}_{1-x}\text{As}$ -based photonic-crystal-slab line-defect waveguide. As a result, we find that the Raman scattering efficiency is pronouncedly enhanced as the signal wavelength approaches the band edge. Comparison of the result with theoretical prediction reveals that the enhancement should reflect increase of the photon density of states in a divergent manner, which is characteristic of a one-dimensional system.

DOI: [10.1103/PhysRevA.78.011805](https://doi.org/10.1103/PhysRevA.78.011805)

PACS number(s): 42.70.Qs, 78.30.-j, 78.70.-g

Spontaneous emission of light (SEL) is not an intrinsic property of atoms, but its rate is determined by interaction with the electromagnetic field, as was first pointed out in 1947 by Purcell [1]. Namely, the rate at a given frequency in a given direction is proportional to the relevant photon density of states (DOS). Consequently, in some special cases, SEL at a particular frequency is expected to be inhibited in all directions, or enhanced in a specific direction. The first experimental evidence was provided in 1983 by placing a Rydberg atom in an optical cavity [2]. For exploiting the above issue, photonic crystals (PhCs) are particularly suited because the photon DOS can be controlled to a considerable extent freely. Recently, it was demonstrated that SEL at particular frequencies in a three-dimensional (3D) PhC is suppressed in all directions [3–5], and that in a PhC slab is suppressed in all two-dimensional (2D) directions [6]. The former phenomenon makes radiative lifetime τ_r of this transition longer where $(\tau_r)^{-1} = A$ (Einstein's A constant).

As for enhancement, it is reported that the SEL at a frequency near the band gap is enhanced in a one-dimensional (1D) PhC [7–10] and in a specific direction in 2D PhC slabs [11–13]. Despite these works, generally speaking, it is not easy to experimentally show that the SEL rate increases in proportion to theoretical DOS when measured as a function of frequency in a range including a band gap. This is because the rate in a certain direction depends not only on those rates in all other directions, but also on the nonradiative lifetime τ_{nr} , so that it depends on both sample quality and temperature. Similar to the SEL, the probability of Raman scattering (RS) by molecular vibration and phonon should also be inhibited or enhanced in a particular direction in PhC slabs [14,15]. So, RS should provide an alternative method for studying Purcell's issue, which was first proposed by Gaponenko [15]. Here we focus on enhancement of RS light. In the case of RS, the concept of the total lifetime of the excited electronic state relevant to the SEL case is not involved. This fact makes the situation very simple. Another advantage of RS is that, unlike the SEL case, there is no need to use a special light source embedded in a sample, because signal (RS) wavelength is easily altered by varying excitation wavelength.

As for DOS, the DOS of electronic state is well known to diverge at Γ point and at the band edge in the first Brillouin zone for a one-dimensional (1D) system [16]. Physically, the same behavior is expected also for the photon DOS. In contrast, the DOS never diverges at the above singular points in both 2D and 3D systems. The purpose of this work is to experimentally demonstrate that the RS efficiency η_R increases in proportion to the photon DOS in model PhC waveguide, for which the photon DOS is known, and thereby, to establish that RS is an alternative method for studying Purcell's issue. Here we note that in the case of a mesoscopic system, strictly speaking, the local DOS, not the conventional DOS, is responsible for light emission [7,15].

We studied η_R of RS caused by optical phonon in an $\text{Al}_x\text{Ga}_{1-x}\text{As}$ -based PhC-slab line-defect waveguide (WG), which is regarded as a quasi-ideal 1D structure. We made measurements for the single guided-mode band of the WG around the signal wavelength of 1600 nm. In this paper we report that η_R increases remarkably, as the wavelength approaches the band edge, and that the observed behavior of η_R agrees well with the theoretical one.

We used a sample of the air-hole type of PhC-slab WG with single-line-defect (W1), which is surrounded by 10 rows of air holes on both sides. Specifically, those samples were fabricated such that a single row of air holes are missing along the Γ - K direction in a prototype $\text{Al}_{0.18}\text{Ga}_{0.82}\text{As}$ PhC slab with 2D triangular lattice structure, which is suspended in air (air-bridge type) [17]. The lattice constant a , thickness d , and hole diameter r are 452, 260, and 120 nm, respectively. The slab plane is normal to $\langle 001 \rangle$ of the cubic AlGaAs , and the light propagation direction is along $\langle 110 \rangle$. We prepared a WG in such a form that the two end facets are equipped with a microlens of half-disk shape for efficient coupling of light to an optical fiber [18]. The sample length L is ~ 1.0 mm.

Figure 1 shows the calculated band dispersion of TE-polarized line-defect modes. There is a frequency range in which the single band of TE-polarized guided mode with even symmetry exists below the air light line. Figure 2 shows the transmittance spectrum measured in the corresponding

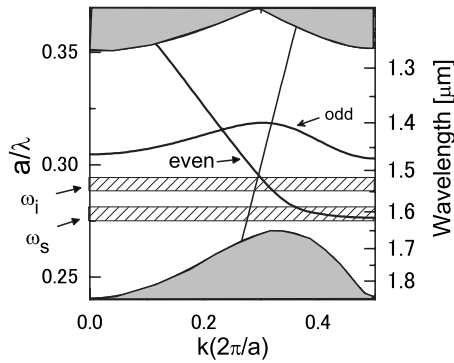


FIG. 1. The theoretical line-defect bands, where ω_i and ω_s are the frequencies of incident and scattered lights, respectively, a is the lattice constant and k is the magnitude of wave vector. The modes in the region below the air light line (shown as a straight line), are guided modes of even symmetry.

frequency range [18]. The spectral region from 1.51 to 1.63 μm corresponds to the above-mentioned range. The observed bandwidth of $\sim 300\text{ cm}^{-1}$ is of the magnitude similar to the present phonon frequencies.

We observed the Stokes Raman signal in the above range in the forward scattering geometry. As an excitation source, we employed a cw wavelength-tunable laser diode (LD). The TE-polarized light of the LD was first coupled to a polarization-preserving single-mode optical fiber, the opposite side of which was polished to be in a form of a lens [18]. Then, using a small lens, the output light from the fiber was coupled to the microlens edge of a PhC WG. The coupled power inside the WG is $\sim 0.2\text{ mW}$. The output lights from the WG were picked up by using a lens and were coupled to another identical fiber. The signal light passed through the filter and was detected with a cooled multichannel InGaAs detector [19], while the excitation laser was blocked by the filter.

Figure 3(a) shows typical Stokes Raman spectra, where RS signals due to the longitudinal (LO) and transverse (TO) optical phonon of AlGaAs are clearly observed with energy shift of 289 and 271 cm^{-1} , respectively [20]. We find that the observed signal intensity varies noticeably with varying laser wavelength in a range covering the band edge, while keeping the coupled power of the laser constant. Figure 3(b) shows a

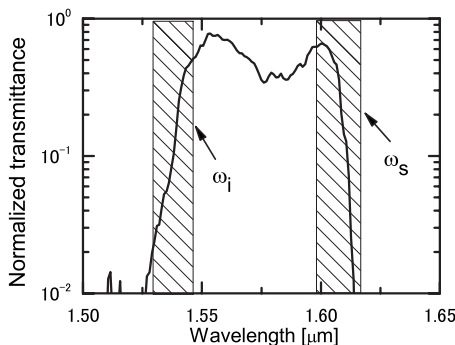


FIG. 2. The observed transmittance spectrum in a range including the guided mode region. The hatched areas show the range in which ω_i and ω_s are varied, respectively.

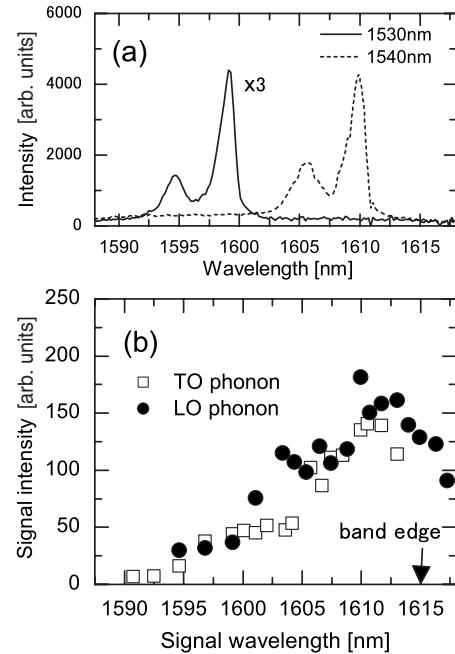


FIG. 3. (a) Typical examples of Raman-scattering spectrum where the solid and dotted lines denote the spectrum observed by using excitation laser of 1530 and 1540 nm in wavelength, respectively. The spectral shift is 289 and 271 cm^{-1} for LO and TO mode, respectively. (b) Variation of signal intensity (relative) as a function of signal wavelength.

plot of the signal intensity (relative) versus the signal wavelength; obvious experimental corrections were made to the data.

From the above data, let us estimate variation of the intrinsic η_R^{ex} value with signal wavelength. Suppose a WG sample has a parallel-piped form with a cross-section area A_{eff} and a length L along the z axis. The signal intensity $I_s(z)$ [the subscript i (S) refers to incident (signal) light] at z obeys the equation,

$$dI_s(z)/dz = -\gamma_s I_s(z) + \alpha I_i(0) \exp(-\gamma_i z), \quad (1)$$

where $I_i(0)$ and $\gamma_S(\gamma_i)$ are the intensity at the input edge, and the attenuation constant at the signal (incident) wavelength, respectively, and α ($\alpha = \eta_R$) is the effective RS coefficient [21], for which the mode overlap with respect to the electric field between incident and signal lights is considered. From Eq. (1) the intensity $I_s(L)$ at the output edge of the sample is expressed as

$$I_s(L) = \alpha I_i(0) L_{\text{eff}}, \quad (2)$$

$$L_{\text{eff}} = \frac{\exp(-\gamma_s L) - \exp(-\gamma_i L)}{\gamma_i - \gamma_s}, \quad (3)$$

which indicates that the $\eta_R(\alpha)$ value is L_{eff} dependent. So, by multiplying $[I_s(L)/I_i(0)]_{\text{ob}}$ by L_{eff}^{-1} , we have estimated the intrinsic η^{ex} value, which is to be compared with the theoretical one. In estimating γ_s from measured transmittance for evaluating L_{eff} 's, we assume that decrease of transmittance with approaching the band edge is caused solely by group

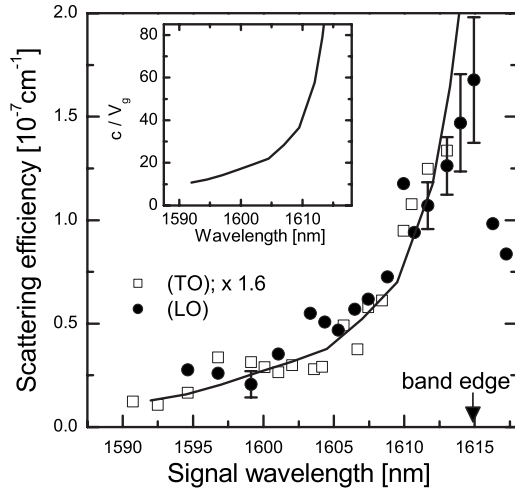


FIG. 4. Variation of the observed scattering efficiency with signal wavelength. The solid curve is the theoretical variation, which is obtained as being variation of c/V_g shown in the inset, multiplied by a constant. The scale of the abscissa is the signal wavelength for LO (circle) and TO (square) phonon.

velocity (V_g)-dependent propagation loss [22]. Figure 4 displays variation of η_R thus estimated with signal wavelength, where η_R clearly increases as the wavelength approaches the band edge.

In order to elucidate the origin of the above behavior of η , let us derive a theoretical formula for spontaneous RS in the quasi-ideal 1D system. It is well known that the Raman transition probability per unit time can be derived quantum mechanically in terms of the second-order time-dependent perturbation or from Fermi's golden rule [23]. The result for the 3D case is known as the so-called Kramers-Heisenberg formula [23,24]. The derivation in the 1D case is rather simple; note that SEL in the quasi-ideal 1D case has already been derived for a microwave metallic WG [25]. Let both laser and signal beams belonging to the respective guided modes propagate along the sample of the form already introduced.

One laser photon is transformed into one scattered (signal) photon. Then, the transition probability τ^{-1} per unit time for one molecule or unit cell in a volume V ($V=L \times A_{\text{eff}}$) is derived microscopically in a way similar to the 3D case [24,26]. Substituting the 1D DOS, $D_1(\omega)$ per unit length, which is given by

$$D_1(\omega)d\omega = D_1(k)\left(\frac{dk}{d\omega}\right)d\omega = \left(\frac{1}{\pi}\right)\left(\frac{dk}{d\omega}\right)d\omega \quad (4)$$

into τ^{-1} , we may have the following relation for η^h :

$$\begin{aligned} \eta^h &\equiv \left(\frac{1}{L}\right)\frac{I_s(L)}{I_i(0)} = \frac{N}{V}\hbar\omega_s\left(\frac{1}{\tau}\right) \\ &= \left(\frac{N}{V}\right)\left(\frac{1}{A_{\text{eff}}}\right)\left(\frac{e^4}{2\varepsilon_0^2\hbar^2}\right)\omega_s^2|M_{SRE}|^2\left(\frac{1}{V_g^S}\right)\left(\frac{1}{V_g^i}\right), \end{aligned} \quad (5)$$

where M_{SRE} denotes the transition matrix element expressed in terms of r -matrix elements (r ; position vector), \hbar is the Planck constant, e electron charge, ε_0 the vacuum dielectric constant, N the number of unit cell contained in V , and ω_s is

angular frequency. In deriving the above equation, we used the relation $I=(V_g\hbar\omega)(nV^{-1})$, where n is the photon number. Note that $(V_g^S)^{-1}$ in Eq. (5) comes from the photon DOS proportional to $(dk/d\omega)_S$, whereas $(V_g^i)^{-1}$ comes directly from group velocity of laser. Equation (5) indicates that η_R^h becomes larger as the band edge is approached, because the DOS at signal wavelength increases in a divergent manner through $(dk/d\omega)=(V_g^S)^{-1}$: Note that variation of V_g^i is small in a measured wavelength range. For comparison, variation of η_R^h with signal wavelength is also shown in Fig. 4. Since η_R^h should vary in the same manner as c/V_g^S , we have shown the curve of c/V_g^S multiplied by a constant as the variation of η_R^h , where the constant is adjusted such that data points in a shorter wavelength range are best fit to the η_R^h curve; V_g^S 's are calculated from the slope of the guided-mode band shown in Fig. 1. The comparison reveals that agreement between variations of η^{ex} and η^h is good in a range below ~ 1613 nm, but beyond this range the discrepancy becomes larger as the wavelength approaches the band edge. Evidently, the large experimental error is responsible for this discrepancy.

Now let us discuss the result. First, we discuss the validity of the above comparison of η_R . Theoretically, variation of η_R^h is also contributed partly from another factor, i.e., the variation of the mode overlap already described between the incident and signal lights, separated by the phonon frequency [27]. Although two modes belong to the same band, the extent of this overlap is subject to change to some extent, by varying the signal wavelength, in particular, at wavelengths close to the band edge. We have ignored this variation by postulating that this factor causes a smaller correction to the increase of η_R due to $(V_g^S)^{-1}$. Note that this correction does not influence the present relative comparison between η^{ex} and η^h , since this factor is similarly included in both of them. Here we briefly mention that the divergent increase of the present DOS should be expressed as $D(\omega_S)=a(\omega_S-\omega_c)^{-(1/2)}$ where a is a positive constant and ω_c is the frequency at the band edge; note that this is the well-known frequency dependence of the electronic DOS around Γ point in the 1D semiconductor quantum wire [16].

Thus far we have experimentally demonstrated that the RS efficiency η_R is enhanced in proportion to the relevant photon DOS. This demonstration is significant, as we have proved Purcell's issue clearly and quantitatively by using RS measurement for the case of enhancement. In spite of many related reports regarding the SEL [8,14,19–23], such a clear-cut and quantitative demonstration as we have shown above has seldom been reported, as far as we know. The present demonstration has been enabled by making full use of the advantage RS has, and by utilizing a simple variation of photon DOS of single-frequency guided-mode band in the 1D PhC WG.

Finally, we mention some related works using PhCs. Concerning spontaneous RS, a few works have been reported until now [14,15,20]; only experimental work is our previous one [20], where measurement was made at a constant wavelength of 1340 nm for a similar WG of W3 line defect with more complicated guided- and leaky-mode bands. Concerning stimulated Raman scattering (SRS), some works have been reported [27–29], although all of them are theoretical

ones. The work in Ref. [27] among others is related to our present one in spite of the obvious difference of SRS from spontaneous RS. Using the coupled-mode theory, the authors treat the SRS in W1 PhC WGs and show, by calculation, drastic enhancement of the SRS gain by making both the pumping and probe wavelengths coincide with the respective band-edge wavelengths of two different guided-mode bands. In this connection, we make a comment that unlike the SEL case, both RS and SRS involve the photon DOSs at two frequencies. Consequently, both DOSs can contribute, in principle, to enhancement of η_R in the RS case, which has first been pointed out in Ref. [14].

In conclusion, we have observed striking a increase of the RS efficiency due to an optical phonon in a 1D $\text{Al}_x\text{Ga}_{1-x}\text{As}$ -based PhC WG, with making the signal wave-

length approach the band edge. We have found that this increase is correlated with $(V_g)^{-1}$, and thereby reflects the divergent behavior of the photon DOS in the 1D system. Thus, we have demonstrated that RS measurement is an alternative method for studying dependence of the light-emission rate on the photon DOS in a frequency range in such a mesoscopic system as showing the band gap.

We are grateful to Professor K. Ohtaka of Chiba University for valuable discussion, and to Dr. Y. Watanabe of University of Tsukuba for calculating the effective areas. This work was financially supported by a Grant-in-aid for Scientific Research from the Ministry of Education, Science, Sports, Culture, and Technology, and also by NEDO within the framework of a NEDO grant.

-
- [1] E. M. Purcell, Phys. Rev. **69**, 681 (1946).
 [2] R. G. Hulet, E. S. Hilfer, and D. Kleppner, Phys. Rev. Lett. **55**, 2137 (1985).
 [3] E. Yablonovitch, Phys. Rev. Lett. **58**, 2059 (1987).
 [4] S. Ogawa, M. Imada, S. Yoshimoto, M. Okano, and S. Noda, Science **305**, 227 (2004).
 [5] P. Lodahl *et al.*, Nature (London) **430**, 538 (2004).
 [6] M. Fujita, S. Takahashi, Y. Tanaka, T. Asano, and S. Noda, Science **308**, 1296 (2005).
 [7] E. Snoeks, A. Lagendijk, and A. Polman, Phys. Rev. Lett. **74**, 2459 (1995).
 [8] M. D. Tocci, M. Scalora, M. J. Bloemer, J. P. Dowling, and C. M. Bowden, Phys. Rev. A **53**, 2799 (1996).
 [9] E. Viasnoff-Schwoob *et al.*, Opt. Lett. **30**, 2113 (2005).
 [10] E. Viasnoff-Schwoob *et al.*, Phys. Rev. Lett. **95**, 183901 (2005).
 [11] M. Zelsmann *et al.*, Appl. Phys. Lett. **83**, 2542 (2003).
 [12] M. Galli *et al.*, Appl. Phys. Lett. **88**, 251114 (2006).
 [13] M. Kaniber *et al.*, Appl. Phys. Lett. **91**, 061106 (2007).
 [14] M. Inoue and K. Ohtaka, Phys. Rev. B **26**, 3487 (1982).
 [15] S. V. Gaponenko, Phys. Rev. B **65**, 140303(R) (2002).
 [16] N. Peyghambarian, S. W. Koch, and A. Mysyrowicz, *Introduction to Semiconductor Optics* (Prentice Hall, New Jersey, 1993) Chap. IX.
 [17] Y. Sugimoto *et al.*, Opt. Express **12**, 1090 (2004).
 [18] N. Ikeda *et al.*, *Proceedings of the 19th International Conference on Indium Phosphide and Related Materials* (IEEE, Matsue, 2007), p. 484.
 [19] K. Inoue *et al.*, Jpn. J. Appl. Phys., Part 1 **43**, 6112 (2004).
 [20] H. Oda, K. Inoue, N. Ikeda, Y. Sugimoto, and K. Asakawa, Opt. Express **14**, 6659 (2006).
 [21] In the 1D case the dimension of η is cm^{-1} , while in the conventional (homogeneous) 3D case, that is $\text{cm}^{-1}\text{Sr}^{-1}$, because the photon DOS is included; note that in the latter case, the scattered radiation is observed with a certain solid angle in a certain direction.
 [22] In Fig. 2 the transmittance decreases markedly as the wavelength approaches the band edge. In the present sample with a microlens, it is revealed that unlike the case of cleaved edges, the coupling loss is constant except for a narrow wavelength region very close to the gap.
 [23] R. Loudon, Adv. Phys. **13**, 423 (1964).
 [24] R. Loudon, *The Quantum Theory of Light* (Clarendon, Oxford, 1973), Chaps. X and XII.
 [25] J. P. Wittke, RCA Rev. **36**, 655 (1975).
 [26] Y. R. Shen, *The Principles of Nonlinear Optics* (Wiley, New York, 1984), Chap. X.
 [27] J. E. McMillan, X. Yang, N. C. Panoiu, R. M. Osgood, and C. W. Wong, Opt. Lett. **31**, 1235 (2006).
 [28] R. G. Zaporozhchenko, S. Ya Killin, and A. G. Smirnov, Quantum Electron. **30**, 997 (2000).
 [29] L. Florescu and X. Zhang, Phys. Rev. E **72**, 016611 (2005).